Redox Biology 34 (2020) 101523

Contents lists available at ScienceDirect

Redox Biology

journal homepage: www.elsevier.com/locate/redox

# NLRP3 inflammasome-mediated pyroptosis contributes to the pathogenesis of non-ischemic dilated cardiomyopathy

Cheng Zeng[a,1], Fengqi Duan[a,1], Jia Hu[a], Bin Luo[c], Binlong Huang[b], Xiaoying Lou[d], Xiuting Sun[e], Hongyu Li[f], Xuanhong Zhang[a], Shengli Yin[b,**], Hongmei Tan[a,g,*]

[a] Department of Pathophysiology, Zhongshan School of Medicine, Sun Yat-sen University, Guangzhou, 510080, China
[b] Department of Cardiac Surgery, The First Affiliated Hospital of Sun Yat-sen University, Guangzhou, 510080, China
[c] Department of Forensic Medicine, Zhongshan School of Medicine, Sun Yat-sen University, Guangzhou, 510080, China
[d] Department of Pathology, The Sixth Affiliated Hospital of Sun Yat-sen University, Guangzhou, 510655, China
[e] Department of Cardiology, The First Affiliated Hospital of Sun Yat-sen University, Guangzhou, 510080, China
[f] Laboratory Animal Center, Sun Yat-sen University, Guangzhou, 510080, China
[g] Guangdong Engineering & Technology Research Center for Disease-Model Animals, Sun Yat-sen University, Guangzhou, 510080, China

ARTICLE INFO

*Keywords:*
Dilated cardiomyopathy
Heart failure
NOX
NLRP3 inflammasome
Pyroptosis
Mitochondrial fission

ABSTRACT

Dilated cardiomyopathy (DCM) is one of the most common causes of heart failure, and the underlying mechanism remains largely elusive. Here we investigated whether NLRP3 inflammasome-mediated pyroptosis contributes to non-ischemic DCM and dissected the underlying mechanism. We found that hyper activated NLRP3 inflammasome with pyroptotic cell death of cardiomyocytes were presented in the myocardial tissues of DCM patients, which were negatively correlated with cardiac function. Doxorubicin (Dox)-induced DCM characterization disclosed that NLRP3 inflammasome activation and pyroptosis occurred in Dox-treated heart tissues, but were very marginal in either *NLRP3*$^{-/-}$ or *caspase-1*$^{-/-}$ mice. Mechanistically, Dox enhanced expressions of NOX1 and NOX4 and induced mitochondrial fission through dynamin-related protein 1 (Drp1) activation, leading to NLRP3 inflammasome-mediated pyroptosis in cardiomyocytes via caspase-1-dependent manner. Conversely, both inhibitions of NOX1 and NOX4 and Drp1 suppressed Dox-induced NLPR3 inflammasome activation and pyroptosis. The alterations of NOX1 and NOX4 expression, Drp1 phosphorylation and mitochondrial fission were validated in DCM patients and mice. Importantly, Dox-induced Drp1-mediated mitochondrial fission and the consequent NLRP3 inflammasome activation and pyroptosis were reversed by NOX1 and NOX4 inhibition in mice. This study demonstrates for the first time that cardiomyocyte pyroptosis triggered by NLRP3 inflammasome activation via caspase-1 causally contributes to myocardial dysfunction progression and DCM pathogenesis.

## 1. Introduction

Dilated cardiomyopathy (DCM) is defined by the presence of left ventricular dilatation and contractile dysfunction, in the absence of abnormal loading conditions and severe coronary artery disease [1]. DCM is one of the most common causes of heart failure (HF) and the most common indication for heart transplantation worldwide [1]. Mechanisms underlying DCM are very complicated and largely unclear, including inflammation and apoptosis, which lead to cell death and ventricular remodeling, and finally contribute to ventricular dilatation and HF. Loss of cardiomyocytes due to apoptosis is believed as the main contributor to progressive myocardial dysfunction in DCM [2–4].

Pyroptotic cell death or pyroptosis was first identified as a pro-inflammatory programmed cell death in *Salmonella*-infected macrophages [5], and has been proved crucial for controlling microbial infections. Accumulating evidence suggests that pyroptosis may contribute to a range of diseases, including autoimmune diseases, diabetes mellitus, nervous system-related diseases and cardiovascular diseases [6,7].

* Corresponding author. Department of Pathophysiology, Zhongshan School of Medicine, Sun Yat-sen University, #74, Zhongshan Road 2, Guangzhou, Guangdong, 510080, China.
** Corresponding author. Department of Cardiac Surgery, the First Affiliated Hospital of Sun Yat-sen University, #58, Zhongshan Road 2, Guangzhou, Guangdong, 510080, China.
*E-mail addresses:* yinshl@mail.sysu.edu.cn (S. Yin), tanhm@mail.sysu.edu.cn (H. Tan).
[1] These authors contributed equally to this work.

https://doi.org/10.1016/j.redox.2020.101523
Received 21 February 2020; Received in revised form 18 March 2020; Accepted 24 March 2020
Available online 30 March 2020

However, to date, whether pyroptosis involves in the cell loss and progressive myocardial dysfunction of DCM is still unknown. There is still no *in vivo* evidence of cardiomyocytes pyroptosis in human heart tissues.

Pyroptosis is identified as inflammatory caspases (mainly caspase-1)-dependent programmed cell death, and closely associated with the activation of inflammasome. NLRP3 inflammasome is the well-known inflammasome and has been identified primarily in monocytes and macrophages, but recent studies demonstrate that NLRP3 inflammasome is activated in other type of cells such as cardiomyocyte [8]. NLRP3 inflammasome formation in cardiomyocytes has potential to activate caspase 1 and induces pyroptosis [9–11]. NLRP3 inflammasome activation generally includes two processes: a priming event that induces transcription of NLRP3 and precursors of caspase-1 (pro-caspase-1) and IL-1β (pro-IL-1β) via toll-like receptor (TLR)/NF-κB signaling, and a subsequent assembly of NLRP3 with the adaptor protein apoptosis-associated speck-like protein containing a caspase recruitment domain (ASC) and pro-caspase-1. This assembly leads to autocleavage of pro-caspase-1, then mediates the maturation and secretion of pro-inflammatory cytokines such as IL-1β and IL-18 [12]. In addition, caspase-1 can cleave gasdermin D (GSDMD) to yield an N-terminal cleavage product (GSDMD-NT), which induces pyroptosis by forming plasma membrane pores [13]. The activation of NLRP3 inflammasome has been linked to key cardiovascular risk factors, including hyperlipidemia, diabetes, obesity and hyperhomocysteinemia [6], and an enhanced inflammatory response is frequently observed in DCM patients [14,15], however, whether NLRP3 inflammasome influences DCM remains unidentified so far.

Acquired causes of DCM include myocarditis and exposure to alcohol, drugs and toxins, and metabolic and endocrine disturbances [1]. Doxorubicin (Dox), a kind of anthracycline antibiotics with a broad spectrum of anti-tumor activity, is reported to induce DCM in patients exposed to Dox [16]. Animal model of DCM is established by Dox and used in the study of DCM [17–19]. Studies demonstrate that inflammation and apoptosis are involved in Dox-induced cardiomyopathy [20,21], however, whether the activation of NLRP3 inflammasome and pro-inflammatory pyroptosis contribute to Dox-induced DCM remains elusive.

The current study aims to investigate whether pyroptosis occurs in heart tissues of DCM patients and mice and contributes to the progressive myocardial dysfunction, and dissect the underlying mechanism.

## 2. Materials and methods

### 2.1. Reagents and antibodies

Dox and GKT137831 (specific dual NOX (nicotinamide adenine dinucleotide phosphate (NADPH) oxidase) 1 and NOX4 inhibitor) were obtained from Selleck Chemicals (Houston, USA). Diphenyleneiodonium chloride (DPI) (NOX inhibitor), N-acetyl-L-cysteine (NAC) and mitoTEMPOL (mitochondria-targeted antioxidant agent) were purchased from Sigma-Aldrich (St Louis, Mo, USA). MCC950 (NLRP3 inflammasome inhibitor) and Mdivi-1 were purchased from MedChem Express (New Jersey, USA). *Z*-YVAD-FMK (YVAD), specific caspase-1 inhibitor, was purchased from Santa Cruz Biotechnology (California, USA). Cell culture reagents were obtained from Invitrogen (Carlsbad, CA, USA). Primary antibodies information (name, company, catalogue number, molecular weight) is shown in Supplemental Table 1. All other reagents were from Sigma unless stated otherwise.

### 2.2. Bioinformatic tools

All expression profiling data analyzed in this study were downloaded from GENE EXPRESSION OMNIBUS (GEO, http://www.ncbi.nlm.nih.gov/geo). Data from GEO series **GSE84796** and **GSE111544** was analyzed using Gene Set Enrichment Analysis (GSEA). The differentially expressed genes in myocardial tissues between the DCM patients and healthy controls were subjected to GO analysis performed with DAVID Bioinformatics Resources 6.7 (http://david.abcc.ncifcrf.gov/) and GSEA analysis with GSEA v2.0.13 software.

### 2.3. Human myocardial and blood samples collection

Human myocardial specimens were collected from the left ventricle free wall of explanted hearts of non-ischemic DCM hearts during cardiac transplantation (n = 9) and brain-dead donor hearts with no history of heart disease (n = 9) at the first affiliated hospital of Sun Yat-sen university. These DCM patients had New York Heart Association (NYHA) functional classification of III-IV and without previous history of hypertension, coronary diseases, valvular heart disease and diabetes mellitus. Heart samples were immediately frozen in liquid nitrogen and stored at −80 °C or fixed in 4% paraformaldehyde for pathological analysis. Blood was collected, and plasma was separated and stored at −80 °C until further analysis. The human study was approved by the Institutional Ethics Committee of the first affiliated hospital of Sun Yat-sen university. The investigation conforms to the principles outlined in the Declaration of Helsinki (Br Med J 1964; ii: 177) with written informed consent from all subjects.

### 2.4. Animal protocol

Wild type (WT), *NLRP3*$^{-/-}$ and *caspase-1*$^{-/-}$ mice (C57BL/6J genetic background, 10 weeks, half of female and male) were obtained from ViewSolid Biotech (Beijing, China). Mice genotype was identified by DNA sequencing technology. To induce DCM, mice were injected with a cumulative dose of 12 mg/kg Dox or equivalent volume of vehicle control via three weekly injections (4 mg/kg i.p. at 0, 7, and 14 days), and subsequent analyses were performed 6 weeks after the first injection [22]. To investigate the role of NOX1 and NOX4 *in vivo*, C57BL/6J mice were fed by gavage with either GKT137831 (dual inhibitor of NOX1 and NOX4) (60 mg/kg) or solvent once a day after the first Dox injection. All mice were kept in certified specific pathogen-free facilities maintained around 24 °C with a 12-h light/dark cycle and free access to food and water. At the end of the experiment, mice were sacrificed; heart tissues and blood samples were collected. Plasma was separated and stored at −80 °C until further analysis. The animal experiments were approved by the Animal Care and Use Committee of Sun Yat-sen University. The investigation conforms to the Guide for the Care and Use of Laboratory Animals published by the US National Institutes of Health (NIH Publication No. 85-23, revised 1996).

### 2.5. Mouse echocardiography

Echocardiography was performed prior to sacrifice using the Visualsonics imaging system (Vivo 2100, Toronto, Canada) with the mice under isoflurane anesthesia as previously described [23]. Echocardiography dimensions (wall thickness and chamber diameter) were obtained using software included in the Visualsonics system.

### 2.6. Histologic analysis

Heart tissues were fixed in 4% paraformaldehyde and then embedded in paraffin. 5 μm sections were collected and subjected to hematoxylin and eosin (HE) and Masson's trichrome staining. For transmission electron microscopic (TEM) observation of ultrastructural changes, myocardial tissues were cut into 1 $mm^3$ tissue blocks and fixed with 3% glutaraldehyde and 4% paraformaldehyde in 0.1 mol/L phosphate buffer. After dehydration with ethanol, the samples were embedded in Durcupan resin for ultra-thin sectioning and TEM examinations.

### 2.7. Cell culture

H9c2 cardiomyocytes were purchased from ATCC (Manassas, VA) and cultured in Dulbecco's modified Eagles medium (DMEM) supplemented with 10% fetal bovine serum (FBS), in a humidified atmosphere with 5% $CO_2$ at 37 °C. After reaching confluence, cells were switched to serum-free medium for 4 h before proceeding with further experiments. Primary neonatal rat ventricular cardiomyocytes (NRVCs) were isolated from 1- to 3-day-old neonatal SD rats as described [24]. Briefly, hearts were minced and dispersed in a series of incubations at 37 °C in Hank's solution containing 1.2 mg/mL pancreatin and 0.14 mg/mL collagenase. After centrifugation, cells were re-suspended in DMEM containing 10% new born calf serum, 100 units/mL penicillin, 100 g/mL streptomycin, and 0.1 mmol/L bromodeoxyuridine. The dissociated cells were pre-plated at 37 °C for 1.5 h. The cells were then diluted and plated in different culture dishes according to the specific experimental requirements. To investigate whether Dox activated NLRP3 inflammasomes *in vitro,* cells were treated with different concentrations of Dox for 24 h. In some experiments, H9c2 cells were pretreated with NAC (1 mmol/L) for 1 h, DPI (20 μmol/L) for 1.5 h, GKT137831 (1 μmol/L) for 1 h, mitoTEMPOL (20 μmol/L) for 0.5 h, or Mdivi-1 (1 μmol/L) for 1 h, and then stimulated with Dox (5 μmol/L) for 24 h. Cells were then processed for further examination such as immunofluorescence microscopy of mitochondrial fission and Western blot.

### 2.8. Immunofluorescent staining (including in vivo pyroptosis and apoptosis analysis)

Immunofluorescent staining protocol was according to our previous report [25]. In brief, heart cryostat sections (4 μm) or cell cultured chamber slides were fixed with 4% paraformaldehyde, blocked with 10% FBS and permeabilized with Triton X-100. The slides were then double immunofluorescent stained with anti-α-actinin (cardiomyocyte marker) and anti-ASC antibodies overnight at 4 °C. After washing with PBS, the cells were incubated with secondary antibodies (Abcam, Cambridge, UK) for 1 h at room temperature. After being mounted with DAPI-containing mounting solution, the slides were subjected to examinations using a confocal laser scanning microscope (LSM780, Zeiss, Germany). For further discrimination the pyroptotic cells from the apoptotic cells in heart tissues, triple-immunostaining of active caspase-1, TdT-mediated dUTP nick end labeling (TUNEL) and α-actinin was performed on heart cryostat sections. Active caspase-$1^+$/$TUNEL^+$ cells were designated as pyroptotic cells, and active caspase-$1^-$/$TUNEL^+$ cells as apoptotic cells. The percentage of $TUNEL^+$, pyroptotic and apoptotic cells were respectively counted in both cardiomyocytes and all types of cells. For each myocardial specimen, 5 fields in each heart section were randomly checked, and the average value was measured. The analysis was performed by a single observer blinded to group allocation.

### 2.9. Mitochondrial morphology analysis

For mitochondrial fission assay, after indicated treatments, cells were incubated with 200 nmol/L MitoTracker Red CMXRos (Molecular Probes, Invitrogen, USA) for 20 min at 37 °C. The structure of mitochondria was viewed by confocal scanning microscopy (LSM780, Zeiss, Germany).

### 2.10. Measurement of intracellular and mitochondrial ROS levels

Intracellular reactive oxygen species (ROS) and mitochondrial ROS were measured by dichloro-dihydro-fluorescein diacetate (DCFH-DA) and MitoSOX™ Red assays (Invitrogen, Carlsbad, CA, USA) based on the manufacturers' instructions, respectively. Briefly, cells were incubated in DMEM with DCFH-DA (10 μmol/L) for 20 min or MitoSOX™ Red (5 μmol/L) for 15 min at 37 °C, and then washed with PBS. The intensity of fluorescence was recorded using a flow cytometer (BECHMAN COULTER, Cytoflex) (at 530 nm for DCFH-DA and 585 nm for MitoSOX).

### 2.11. Flow cytometry analysis for cell pyroptosis

To assess pyroptosis in cardiomyocytes, cells were treated with Dox (5 μmol/L) in the presence or absence of caspase-1 inhibitor YVAD (50 μmol/L) or NLRP3 inhibitor MCC950 (10 μmol/L) for 24 h, or cells were preincubated with GKT137831 (1 μmol/L) or Mdivi-1 (1 μmol/L) for 1 h and then treated with Dox (5 μmol/L) for 24 h. The cells were trypsinized, stained with active caspase-1 and 7-aminoactinomycin D (7-AAD) for 15 min in 37 °C, and then subjected for Flow cytometry (BECHMAN COULTER, Cytoflex) analysis. Active caspase-1 was determined using the FAM-YVAD-FMK caspase-1 detection kit (Cell technology, Mountain View, CA, USA) according to the manufacturer's protocol. 7-AAD stains the core of pyroptotic cells through membrane pore formation. Active caspase-$1^+$/$7\text{-}AAD^+$ cells were defined as pyroptosis population.

### 2.12. LDH release assay

The release of lactate dehydrogenase (LDH) into the supernatant was regarded as an indicator of cytotoxicity. After indicated treatments, culture supernatants were harvested, and the LDH levels were determined using the LDH Release Assay Kit (Nanjing Jiancheng Bioengineering Institute, Jiangsu, China) according to the manufacturer's instruction. The absorbance of samples was measured at 440 nm using a microplate reader (Thermo fisher scientific, Mass, USA).

### 2.13. Western blot analysis

Proteins from human heart tissues, mouse heart tissues or cell lysates were collected. Western blot was performed using standard method. Membranes were incubated with specific antibodies against NF-κB, p-Ser536-NF-κB, NLRP3, Caspase-1, IL-1β, IL-18, GSDMD, NOX1, NOX2, NOX4, dynamin-related protein 1 (Drp1), p-Ser616-Drp1, p-Ser637-Drp1 and β-actin, respectively. Protein bands were analyzed by a ChemiDoc™ Touch Imaging System (Bio Rad, CA, USA). Quantification of band intensity was carried out using Image J software (NIH, Bethesda, MD, USA).

### 2.14. ELISA assay of IL-1β and IL-18

The concentrations of the pro-inflammatory cytokines IL-1β and IL-18 in the plasma of mice or human were determined by the use of commercial ELISA kits (Human or mice sensitive kits for IL-1β and IL-18, MultiSciences Biotech, shanghai, China). Meanwhile, IL-1β in the culture media of H9c2 cells was also measured by ELISA assay (Rat sensitive kits for IL-1β, MultiSciences Biotech, shanghai, China) according to the manufacturer's instruction.

### 2.15. Statistics analysis

Results are expressed as mean ± SD. All *in vitro* experiments were performed at least three times. Correlation analysis was performed by Pearson chi-square test. Statistical comparison between 2 groups was performed via Student's *t*-test (data with normal distribution and homogeneity of variance) or Mann-Whitney test (data not normally distributed or without homogeneity of variance). Statistical comparison among multiple groups was carried out by one-way ANOVA followed by LSD test (data with normal distribution and homogeneity of variance) or Kruskal-Wallis test followed by Dunn's test (data not normally distributed or without homogeneity of variance). Data were analyzed using Graphpad Prism 6.02 software. $P < 0.05$ was considered statistically significant.

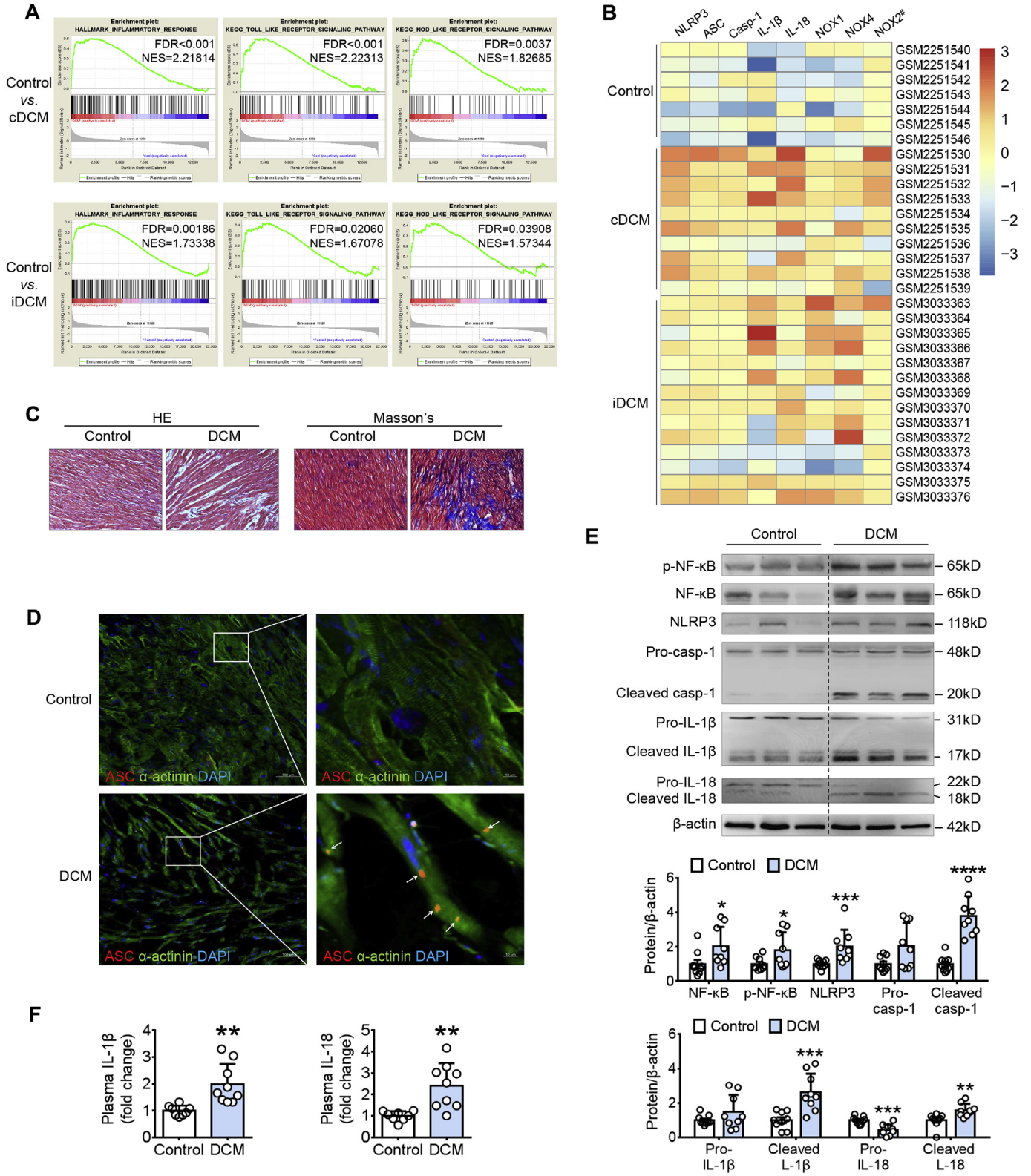


**Fig. 1. NLRP3 inflammasomes are activated in heart tissues from non-ischemic DCM patients**. (A) The enrichment results of inflammatory response, TLR and NLR signature genes in the myocardial tissues of DCM patients (data from GEO data-set **GSE84796** and **GSE111544**) (n = 31). (B) Heatmap showing the expression of NLRP3 inflammasome components, IL-1β, IL-18, NOX1, NOX2 and NOX4 in myocardial tissues of cDCM patients (n = 10), iDCM patients (n = 14) and normal controls (n = 7) (data from GEO data-set **GSE84796** and **GSE111544**). # indicated that control *vs* iDCM, $p > 0.05$. (C) HE and Masson's trichrome staining of heart tissues. (D) Immunofluorescent staining showing ASC specks formation in cardiomyocytes. (E) Representative immunoblots of the indicated proteins in myocardial tissues and the corresponding quantification (n = 9). (F) Plasma levels of IL-1β and IL-18 (n = 9). Casp-1: caspase-1. $*p < 0.05$, $**p < 0.01$, $***p < 0.001$ and $****p < 0.0001$ vs control group.

**Table 1**
Clinical characteristics of DCM patients.

| | DCM1 | DCM2 | DCM3 | DCM4 | DCM5 | DCM6 | DCM7 | DCM8 | DCM9 | |
|---|---|---|---|---|---|---|---|---|---|---|
| Age (years) | 60 | 58 | 52 | 50 | 30 | 39 | 12 | 51 | 42 | 43.8 ± 15.2 |
| Gender male | Y | Y | Y | Y | Y | Y | Y | Y | Y | |
| Prior hypertension | N | N | N | N | N | N | N | N | N | |
| Coronary diseases | N | N | N | N | N | N | N | N | N | |
| Valvular heart disease | N | N | N | N | N | N | N | N | N | |
| Diabetes mellitus | N | N | N | N | N | N | N | N | N | |
| NYHA class | 4 | 3 | 3 | 3 | 3 | 3 | 3 | 4 | 4 | 3.3 ± 0.5 |
| NT-ProBNP (pg/mL) | 6929 | 2057 | 31,263 | 626.2 | 4245 | 1065 | 1621 | 2137 | 409.4 | 5594.7 ± 9841.3 |
| Hemoglobin (g/L) | 109 | 131 | 147 | 115 | 155 | 126 | 136 | 132 | 164 | 135.0 ± 17.9 |
| Hematocrit | 0.453 | 0.394 | 0.426 | 0.347 | 0.358 | 0.365 | 0.412 | 0.382 | 0.497 | 0.404 ± 0.049 |
| Total cholesterol (mmol/L) | 5.7 | 4.8 | 9 | 4.6 | 5.1 | 2.5 | 5.8 | 4.3 | 5.2 | 5.2 ± 1.7 |
| Duration of disease (months) | 240 | 180 | 3 | 108 | 10 | 60 | 8 | 192 | 5 | 89.6 ± 93.6 |
| **Echo-Doppler study** | | | | | | | | | | |
| LVEF (%) | 29 | 12 | 20 | 18 | 25 | 26 | 17 | 20 | 27 | 21.6 ± 5.6 |
| LVESD (mm) | 52 | 86 | 67 | 72 | 59 | 63 | 57 | 90 | 64 | 67.8 ± 12.9 |
| LVEDD (mm) | 60 | 91 | 74 | 79 | 68 | 72 | 62 | 99 | 73 | 75.3 ± 12.8 |
| LAD (mm) | 46 | 49 | 35 | 69 | 55 | 53 | 43 | 69 | 47 | 51.8 ± 11.3 |

Y: yes, N: no, LVEF: left ventricular ejection fraction, LVESD: left ventricular end systolic diameter, LVEDD: left ventricular end diastolic diameter, LAD: left atrial diameter.

## 3. Results

### 3.1. NLRP3 inflammasomes are activated in heart tissues from non-ischemic DCM patients

To check if inflammasome signals are involved in DCM progression, we first performed GSEA using data from DCM patient dataset (**GSE84796** and **GSE111544**). We found that inflammation response, TLR and Nod-like receptor (NLR) pathways were enriched in both chagasic DCM (cDCM) patients and idiopathic DCM (iDCM) patients (Fig. 1A), and expressions of NLRP3 inflammasome/IL-1β axis were significantly higher in DCM hearts than in healthy control (Fig. 1B), indicating that inflammasome are associated to DCM progression [26,27].

To explore whether NLRP3 inflammasome activation is present in DCM hearts, myocardial specimens were collected from non-ischemic DCM patients with end-stage HF and control donors. The patients' clinical and echocardiographic characteristics were summarized in Table 1. Heart lesions were confirmed by HE and Masson's trichrome staining (Fig. 1C). NLRP3 inflammasome was activated as evidenced by ASC specks formation in cardiomyocytes and the cleavage of caspase-1, IL-1β and IL-18 (Fig. 1D–E). Priming of NLRP3 inflammasomes also accompanied DCM progression, as evidenced by the increased expression and phosphorylation of NF-κB in patients with DCM (Fig. 1E). Plasma IL-1β and IL-18 of DCM patients were significantly higher than those of healthy controls (Fig. 1F). All these results strongly indicated that NLRP3 inflammasome is activated in the myocardial tissues of non-ischemic DCM patients and may contribute to cardiac dysfunction.

### 3.2. Pyroptosis is occurred in heart tissues from non-ischemic DCM patients

Given NLRP3 inflammasome activation is closely related to pyroptosis, we further investigated whether pyroptosis was occurred in the myocardium of non-ischemic DCM patients. GSDMD-NT is the executor of pyroptosis, and the cleavage of GSDMD is used as an important indicator for evaluating pyroptosis [13]. Compared to control hearts, GSDMD was cleaved obviously in the myocardial tissues of all nine DCM patients (Fig. 2A), indicating the presence of pyroptosis in all DCM hearts.

To further confirm the presence and extent of pyroptosis in DCM patients, triple-immunostaining of active caspase-1, TUNEL and α-actinin was performed. For each heart section, 5 fields were randomly checked, and 1442 to 2081 cells were counted in DCM patients respectively. Pyroptotic cell death was obviously observed in heart tissues of all nine DCM patients, in contrast, no pyroptotic cell observed in control hearts (Fig. 2B). Interestingly, the number of TUNEL and active caspase-1 double positive cells were less than TUNEL single positive cells, indicating the heart cell death is not totally attributed to pyroptotic cells, but with some apoptotic cells. In patients with DCM, the pyroptotic cells were not evenly distributed, but clustered together (Fig. 2B). Among the TUNEL-positive cell population, the pyroptotic cells were more than apoptotic cells (Fig. 2C), and both pyroptotic and apoptotic cells were majority of cardiomyocytes (Fig. 2D). Importantly, the percentage of pyroptotic cardiomyocytes was significantly higher than the percentage of apoptotic cardiomyocytes in the heart tissue of DCM patients (11.62 ± 5.30 *vs* 7.57 ± 2.86, $p < 0.01$) (Fig. 2C, Table 2), suggesting that pyroptosis may play a more important role than apoptosis in DCM progression. The left ventricular EF was negatively related to TUNEL positive, pyroptotic or apoptotic cardiomyocytes respectively (Fig. 2E), indicating that cardiomyocyte death contributes to the progressive myocardial dysfunction in DCM.

### 3.3. NOX1 and NOX4 are associated to cleavages of caspase-1 and GSDMD in DCM patients

As showed in Supplementary Fig. 1A, ROS pathway was also identified to be closely related with DCM in GEO data-set (**GSE84796** and **GSE111544**). Given that NOXs-derived ROS have potential for activation of NLRP3 inflammasomes [28], we investigated whether NOX expression was related to NLRP3 inflammasomes activation in the myocardial tissues of DCM patients. Immunoblots revealed that expressions of NOX1 and NOX4, but not NOX2, were elevated in DCM hearts, and NOX1 and NOX4 expression were positively correlated with the cleaved caspase-1 and GSDMD-NT in the myocardial tissues of DCM patients (Fig. 3A–D). These results are consistent with those derived from iDCM patient dataset (**GSE111544**) (Fig. 1B; Supplementary Figs. 1B–C). All these data indicated that upregulations of NOX1 and NOX4 might be involved in NLRP3 inflammasome activation and pyroptosis in DCM progression.

### 3.4. NLRP3 inflammasome-mediated pyroptosis via caspase-1 contributes to dox-induced DCM

To further investigate the role of NLRP3 inflammasome and pyroptosis in non-ischemic DCM, DCM model in mice was successfully induced with Dox injection. Dox administration caused increased left ventricular end systolic diameter (LVESD) and left ventricular end diastolic diameter (LVEDD) along with decreased EF, fractional

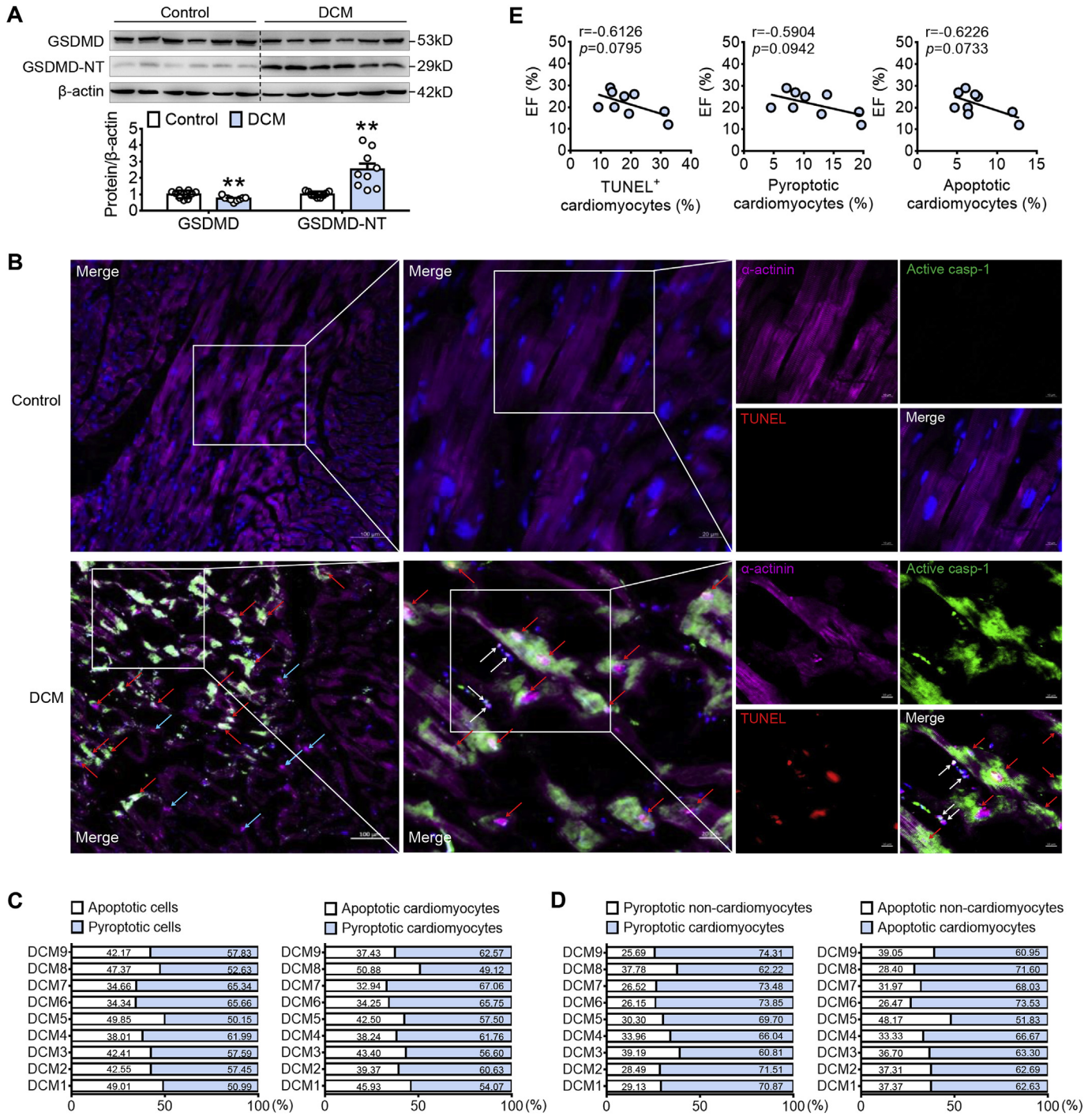


**Fig. 2. Pyroptosis is occurred in heart tissues from non-ischemic DCM patients**. (A) Representative immunoblots and the corresponding quantification of the cleavage status of GSDMD (n = 9). (B) Triple-immunostaining of active caspase-1, TUNEL and α-actinin. Red arrows: pyroptotic cardiomyocytes (active caspase-1$^+$/TUNEL$^+$/α-actinin$^+$ cells), white arrow: pyroptotic non-cardiomyocytes (active caspase-1$^+$/TUNEL$^+$/α-actinin- cells), blue arrows: apoptotic cardiomyocytes (active caspase-1-/TUNEL$^+$/α-actinin$^+$ cells). (C) The ratio of pyroptotic cells to apoptotic cells in all types of cells or in cardiomyocytes (n = 9) and (D) the ratio of cardiomyocytes to non-cardiomyocytes in all pyroptotic cells or apoptotic cells in DCM heart tissues (n = 9). (E) Correlationship of EF with TUNEL positive, pyroptotic and apoptotic cardiomyocytes in DCM patients (n = 9). $^{**}p < 0.01$ *vs* control group. (For interpretation of the references to colour in this figure legend, the reader is referred to the Web version of this article.)

shortening (FS) and ratio of heart weight to body weight (HW/BW) (Fig. 4A–B). Myocardial damage by Dox was comfirmed by HE and Masson's trichrome staining (Fig. 4A). In addition, Dox-induced cardiac dysfunction and myocardial damage were associated to NLRP3 inflammasome activation and pyroptosis, which were evidenced by increased expression of NLRP3, enhanced cleavage of caspase-1, IL-1β, IL-18 and GSDMD in the myocardial tissues (Fig. 4C). Consistent with the results from human DCM patients, priming signal NF-κB, as well as NOX1 and NOX4 expressions were also upregulated by Dox treatment (Fig. 4C). Importantly, either *NLRP3* or *caspase-1* konckout suppressed Dox-induced NLRP3 inflammasome activation and pyroptosis (Fig. 4C), and consequently alleviated Dox-induced cardiac dysfunction and myocardial damage (Fig. 4A–B). These results suggested that NLRP3 inflammasome-mediated pyroptosis via caspase-1 contributes to Dox-

**Table 2**
Percentage of TUNEL$^+$, pyroptotic and apoptotic cardiomyocytes in DCM patients.

| Patient No. | TUNEL$^+$ cardiomyocytes (%) | Pyroptotic cardiomyocytes (%) | Apoptotic cardiomyocytes (%) |
|---|---|---|---|
| DCM1 | 13.15 | 7.11 | 6.04 |
| DCM2 | 32.47 | 19.69 | 12.78 |
| DCM3 | 14.55 | 8.23 | 6.31 |
| DCM4 | 31.25 | 19.30 | 11.95 |
| DCM5 | 17.84 | 10.26 | 7.58 |
| DCM6 | 21.16 | 13.91 | 7.25 |
| DCM7 | 19.38 | 13.00 | 6.38 |
| DCM8 | 9.16 | 4.50 | 4.66 |
| DCM9 | 13.75 | 8.60 | 5.14 |
| Mean ± SD | 19.19 ± 8.03 | 11.62 ± 5.30** | 7.57 ± 2.86 |

**$p < 0.01$ *vs* apoptotic cardiomyocytes.

induced DCM.

### 3.5. Dual inhibition of NOX1 and NOX4 attenuates NLRP3 inflammasome-mediated pyroptosis in DCM

To broaden our observations in DCM patients, we investigated whether NOX1 and NOX4 inhibition could regulate NLRP3 inflammasome activation and pyroptosis. Inhibition of NOX1 and NOX4 with a specific inhibitor, GKT137831, attenuated Dox-induced cardiac dysfunction and myocardial damage (Fig. 5A–B). NLRP3 inflammasome activation and pyroptosis, as well as increased expression of NF-κB, were all inhibited by GKT137831 in Dox-treated heart tissues (Fig. 5C). In parallel with results from western blotting analysis, double immunofluorescent staining showed that Dox-induced ASC specks formation in cardiomyocytes was also attenuated by GKT137831 administration (Fig. 5D). All these indicated that NOX1 and NOX4 contributes to NLRP3 inflammasome activation and related pyroptosis in DCM.

### 3.6. Both NOX1/NOX4-derived ROS and mitochondrial ROS contribute to dox-induced NLRP3 inflammasome activation

Given that ROS plays central role in NLRP3 inflammasome activation [29], we sought to know whether NOX1/NOX4-drived ROS involves in Dox-induced NLRP3 inflammasome activation. We found that Dox promoted expressions of NOX1 and NOX4 to activate NLRP3 inflammasome via ROS-dependent pathway (Supplementary Figs. 2A–D). To further explore the role of NOX1 and NOX4, GKT137831 was used to specifically inhibit NOX1 and NOX4 activity *in vitro*. GKT137831 reduced intracellular ROS level and suppressed Dox-induced NLRP3 inflammasome activation in H9c2 cells, and the efficacy of GKT137831 was comparable to that of a well-known inhibitor of NOXs, DPI (Fig. 6A–B). Similarly, mitoTEMPOL, a mitochondria-targeted antioxidant agent, significantly inhibited Dox-induced mitochondrial ROS accumulation and NLRP3 inflammasome activation (Fig. 6C–D). These results indicated that both NOX1/NOX4-derived ROS and mitochondrial ROS contribute to Dox-induced NLRP3 inflammasome activation.

### 3.7. NOX1 and NOX4 contribute to NLRP3 inflammasome activation through Drp1-mediated mitochondrial fission

To dissect the origin of ROS, we tentatively examined the effect of Dox on mitochondrial morphology and Drp1 phosphorylation. Results showed that Dox induced dramatic mitochondrial fission (small punctuated mitochondria), translocation of Drp1 into mitochondria with an increase in Drp1 phosphorylation at Ser616 (p-Ser616) and a decrease in phosphorylation at Ser637 (p-Ser637) (indicator of Drp1 activation) (Fig. 6E–F). Mdivi-1 (Drp1 inhibitor) significantly blocked Dox-induced mitochondrial ROS accumulation (Fig. 6G). All these results indicated that Drp1-mediated mitochondrial fission was involved in Dox-induced mitochondrial ROS accumulation and NLRP3 inflammasome activation. Interestingly, the alteration of Drp1 phosphorylation, translocation of Drp1 into mitochondria and mitochondrial fission were all inhibited by GKT137831 upon Dox stimulation (Fig. 6E and H), indicating the

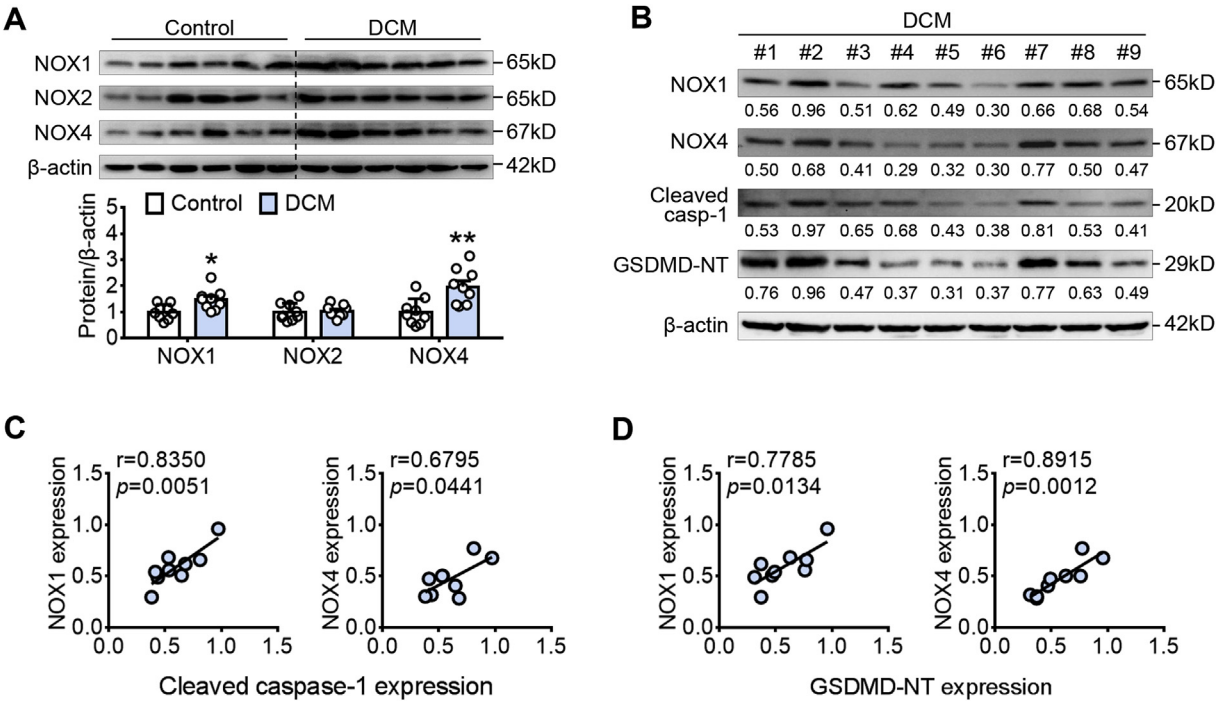


**Fig. 3. NOX1 and NOX4 are associated with the cleavage of caspase-1 and GSDMD in non-ischemic DCM patients**. (A) Representative immunoblots and the corresponding quantification of NOX1, NOX2 and NOX4 (n = 9). (B) Immunoblots of the indicated proteins in myocardial tissues in all nine DCM patients (n = 9). The relative expression level of each protein are quantified and shown under each blots. (C–D) Correlationship of the cleaved caspase-1 (C) or GSDMD-NT (D) with NOX1 and NOX4 in myocardial tissues of DCM patients (n = 9). Casp-1: caspase-1. *$p < 0.05$ and **$p < 0.01$ *vs* control group.

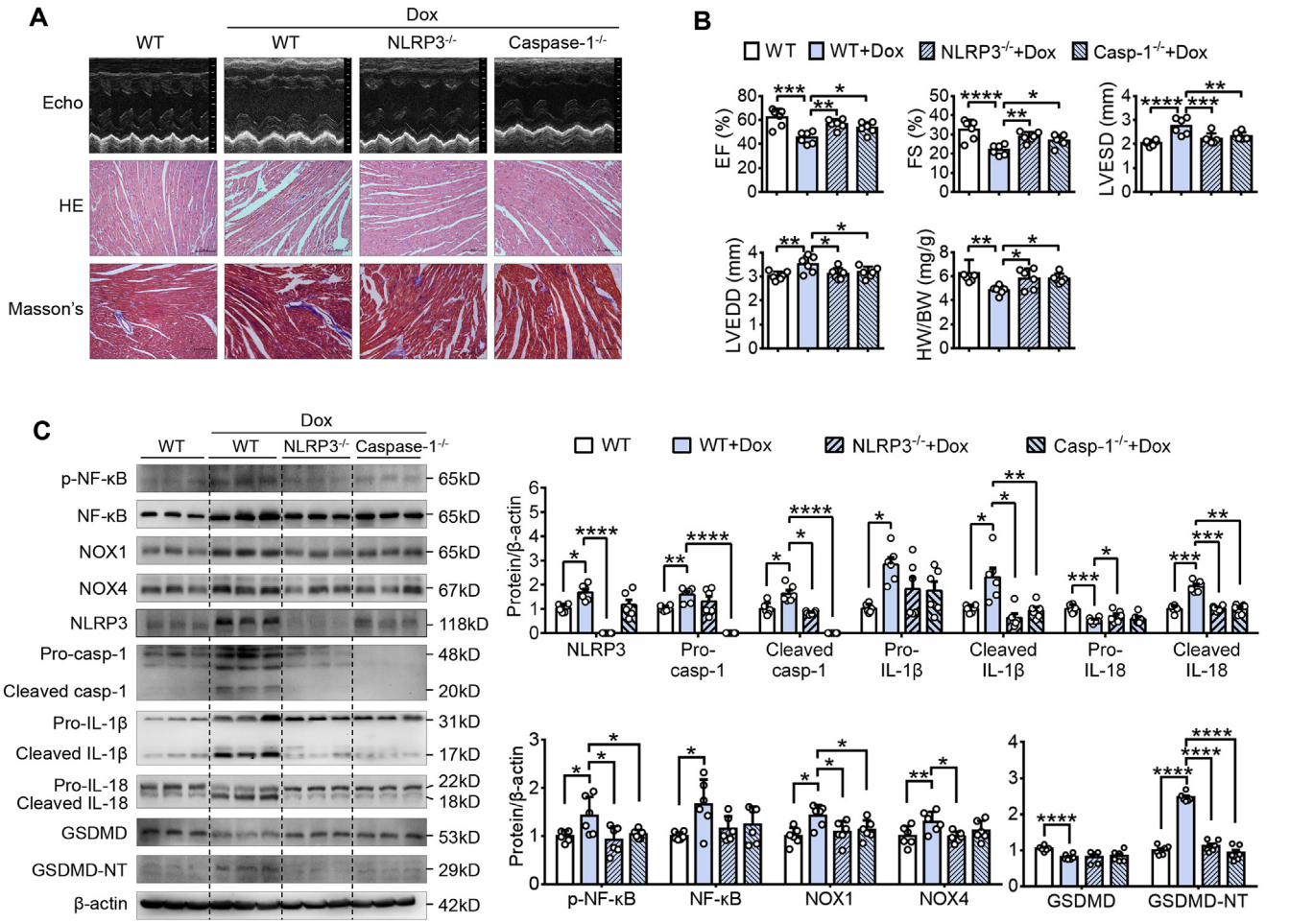


**Fig. 4. NLRP3 inflammasome-mediated pyroptosis via caspase-1 contributes to Dox-induced DCM**. (A) Representative echocardiographic (Echo), HE and Masson's trichrome staining images. (B) Cardiac function index (n = 6). (C) Representative immunoblots and the corresponding quantification of the indicated proteins in myocardial tissues (n = 6). Casp-1: caspase-1. $*p < 0.05$, $**p < 0.01$, $***p < 0.001$ and $****p < 0.0001$.

essential role of NOX1/NOX4 in Drp1-mediated mitochondrial fission.

### 3.8. NOX1 and NOX4 facilitate Drp1 activation and mitochondrial fission in DCM

To confirm the Drp1-mediated mitochondrial fission in heart tissues, we checked Drp1 phosphorylation state and observed that Dox treatment promoted Drp1 activation, which was efficiently inhibited by GKT137831 treatment in heart tissues of mice (Fig. 7A). Changes of Drp1 phosphorylation were accompanied with the increased mitochondrial width, reduced mitochondrial length and mitochondrial length/width ratio in the myocardial tissues of Dox-treated mice, manifesting the very active mitochondrial fission, while these events were significantly attenuated by GKT137831 treatment (Fig. 7B). All results here indicated that Dox induced Drp1 activation and mitochondrial fission in myocardial tissues through NOX1 and NOX4 activation. Similar change in Drp1 phosphorylation was also observed in the myocardial tissues of DCM patients (Fig. 7C). Meanwhile, small spheroid mitochondria were also observed in patients, indicating the very active mitochondrial fission in the heart tissues of DCM patients (Fig. 7D).

### 3.9. Inhibition of NOX1 and NOX4 or Drp1 prevents NLRP3 inflammasome activation and cardiomyocyte pyroptosis

To validate the possible disturbance of DCM via targeting the disclosed signaling, we treated both NRVCs and H9c2 cardiomyocytes with caspase-1 inhibitor YVAD and NLRP3 inhibitor MCC950. During pyroptosis, GSDMD-NT can combine with lipid in the plasma membrane and form large oligomeric pores, leading to the release of cellular contents and positive staining of dead cells, which can be determined by LDH release assay and 7-AAD staining. Contrary to the Dox alone treatment cells, in which include more population of active caspase-1$^+$/7-AAD$^+$ cells, higher LDH release, and more cleavage of caspase-1, IL-18 and GSDMD, both types of inhibitor efficiently interrupted all these events (Fig. 8A–D; Supplementary Figs. 3A–C), suggesting the crucial role of caspase-1 in NLRP3 inflammasome-mediated cardiomyocyte pyroptosis. NLRP3 inflammasome activation and cardiomyocyte pyroptosis by Dox induction were also significantly blocked by GKT137831 and Mdivi-1 (Fig. 8A–D; Supplementary Figs. 3D–F), indicating that targeting both NOX1/NOX4 and Drp1 would be a potential strategy in the type of pyroptosis-sufficient DCM.

## 4. Discussion

To the best of our knowledge, the present study provides the first *in vivo* evidence of cardiomyocyte pyroptosis in human heart tissues. Currently, loss of cardiomyocytes is believed due to apoptosis in DCM. Here, we demonstrate for the first time that hyperactivated NLRP3 inflammasome triggers pyroptotic cell death of cardiomyocytes, which is causally linked to the progressive myocardial dysfunction, culminating in DCM and end-stage HF. These findings uncover a novel and important event in the initiation and progression of DCM and HF. Mechanistically, we disclose for the first time that NOX1 and NOX4

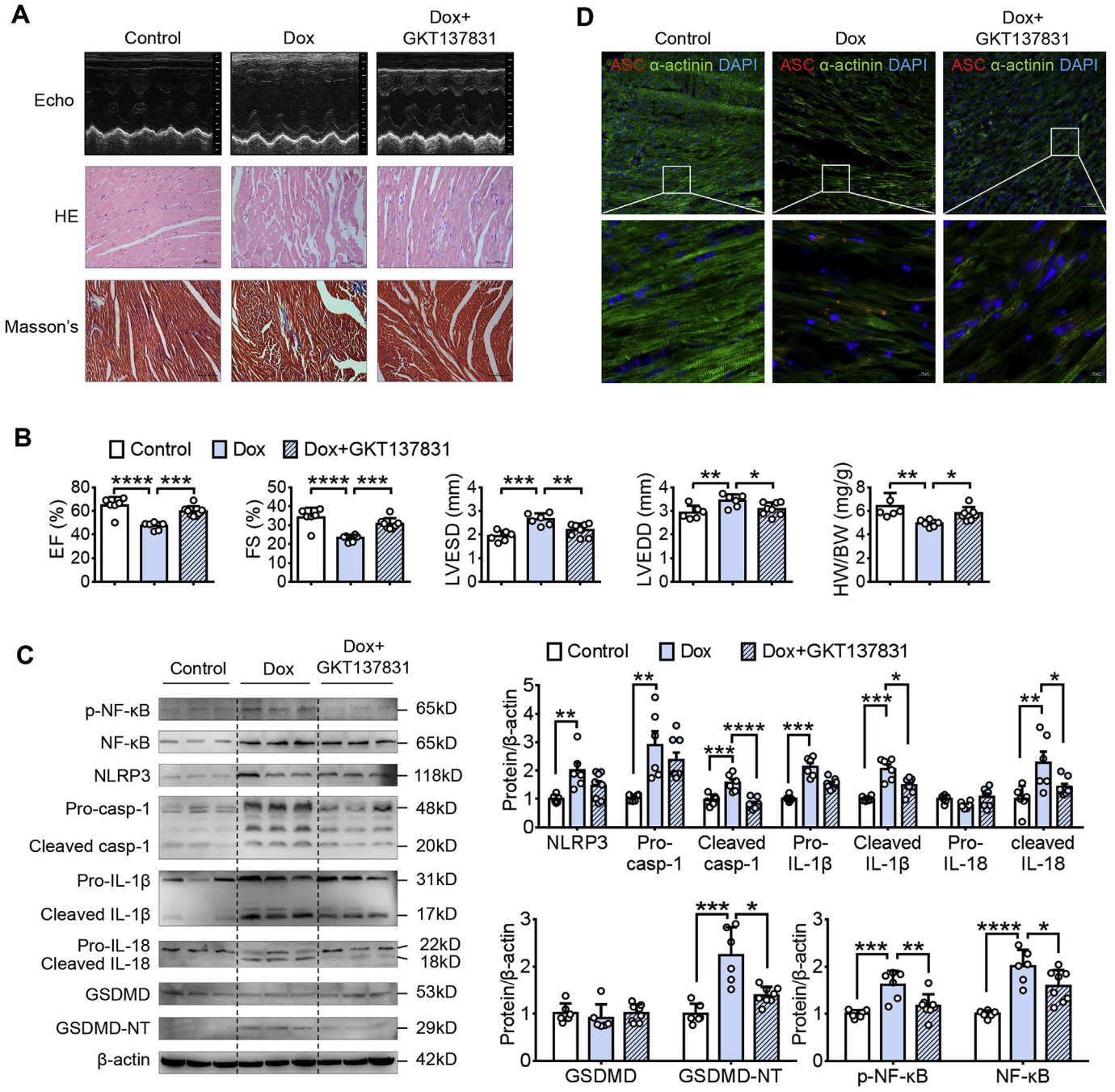


**Fig. 5. Dual inhibition of NOX1 and NOX4 attenuates NLRP3 inflammasome-mediated pyroptosis in DCM**. (A) Representative echocardiographic (Echo), HE and Masson's trichrome staining images. (B) Cardiac function index (n = 6–8). (C) Representative immunoblots and the corresponding quantification of the indicated proteins (n = 6–8). (D) Immunofluorescent staining showing ASC specks formation in cardiomyocytes. Casp-1: caspase-1. *$p < 0.05$, **$p < 0.01$, ***$p < 0.001$ and ****$P < 0.0001$.

facilitate Drp1-mediated mitochondrial fission, render ROS accumulation and the consequent NLRP3 inflammasome activation and cardiomyocyte pyroptosis in DCM. Analyses of the DCM patient tissues also validate these results. Moreover, inhibition of NOX1 and NOX4 successfully reverses the cardiomyopathy in mice. Therefore, targeting NLRP3 inflammasome activation or blocking pyroptosis of cardiomyocytes is potential therapeutical strategy for chronic cardiomyopathy and HF.

Narula et al. performed the first histochemical and histologic analysis in the myocardial tissues of patients with iDCM and indicated that apoptosis is one of the mechanisms leading to end-stage heart disease [2]. Thereafter, accumulating evidence suggests that cardiomyocyte apoptosis is an important cause of cell loss in patients with DCM, leading to the progressive myocardial dysfunction, culminating in end-stage HF [3,4,30]. Consistent with previous study which identified that apototic index (percentage of TUNEL positive-staining cardiomyocytes) ranged from 5.0 to 35.5 in four iDCM patients [2], we found that the percentage of TUNEL positive-staining cardiomyocytes ranged from 9.16 to 32.47 in nine non-ischemic DCM patients. Previously, apoptotic cell death was identified by TUNEL-staining. Emerging evidence has demonstrated that both pyroptotic and apoptotic cells share some common features, including DNA fragmentation which can be labeled by TUNEL-staining [31,32]. Therefore, cells undergoing pyroptotic cell death also stain positively with TUNEL. Given that pyroptosis is

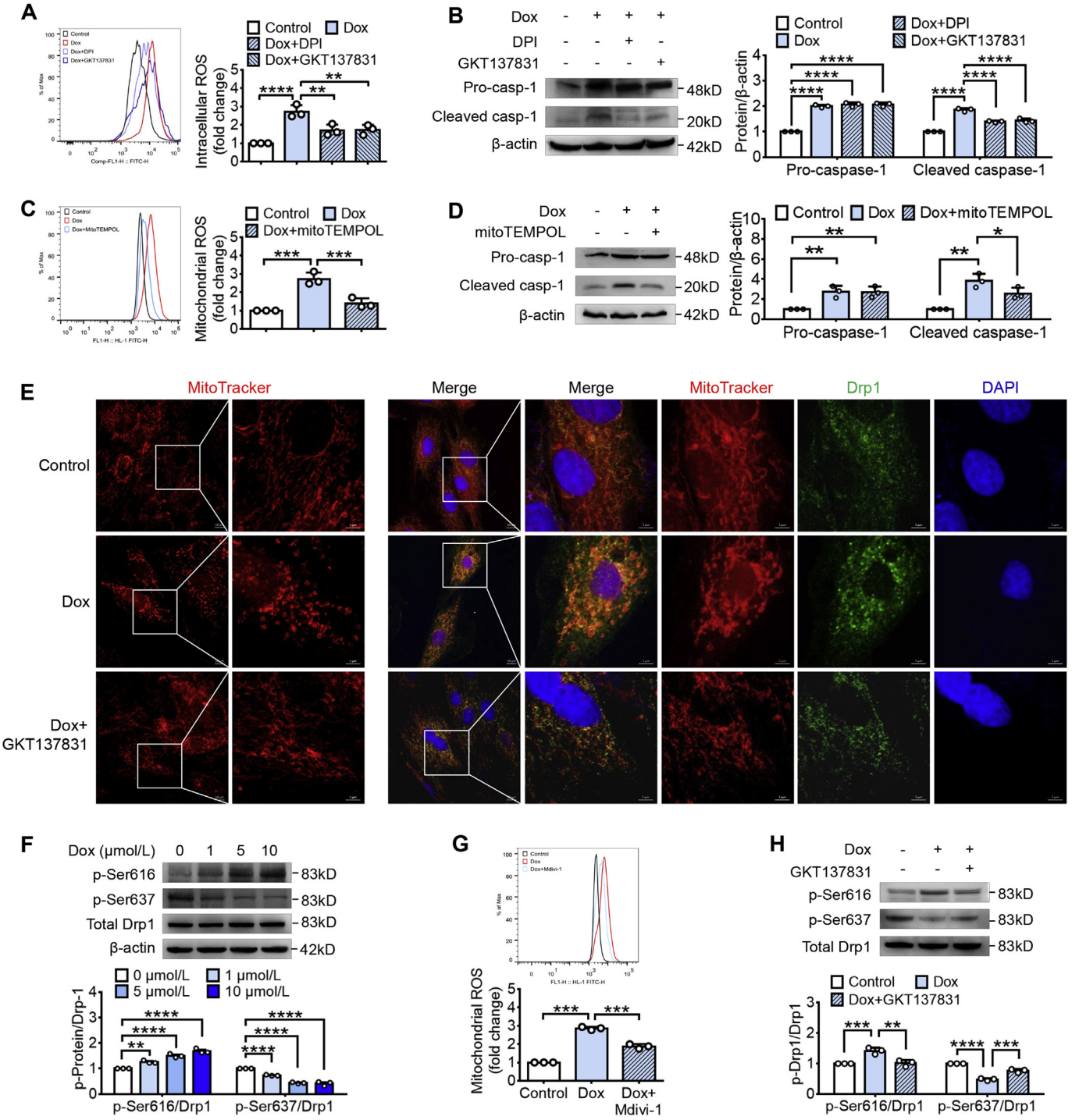


**Fig. 6. NOX1 and NOX4 contribute to NLRP3 inflammasome activation through Drp1-mediated mitochondrial fission**. (A, C and G) Representative flow cytometric image and quantitative analysis of intracellular ROS levels (A) or mitochondrial ROS levels (C and G) (n = 3). (B, D, F and H) Representative immunoblots and the corresponding quantification of the indicated proteins in H9c2 cells (n = 3). (E) Representative confocal microscopic images of MitoTracker and Drp1. Casp-1: caspase-1. $^{**}p < 0.01$, $^{***}p < 0.001$ and $^{****}p < 0.0001$.

characterized as the inflammatory caspases (mainly caspase-1)-dependent programmed cell death, to distinguish the pyroptotic cells from the apoptotic cells, we validated the pyroptotic cells with the cleaved GSDMD status and disclosed that the pyroptotic cell has active caspase-1 and TUNEL double positive staining, wheras the apoptotic cell has active caspase-1$^{-}$/TUNEL$^{+}$ feature. We also found that pyroptotic cells were not uniformly distributed throughout the heart section, but clustered together irregularly. Importantly, both pyroptotic and apoptotic cells are mainly composed of cardiomyocytes, indicating that the cardiomyocytes death is the key cause of DCM. Our data also indicated that pyroptosis may play a more important role than apoptosis in DCM progression, as the percentage of pyroptotic cardiomyocytes is significantly higher than that of apoptotic cardiomyocytes. More importantly, the percentage of pyroptotic cardiomyocytes is positively correlated to cardiac dysfunction of DCM patients, indicating that cardiomyocyte pyroptosis might be an important cause for deterioration in cardiac function. Taken together, our findings uncover a novel and important pyroptosis effect in the pathogenesis of DCM, and highlight

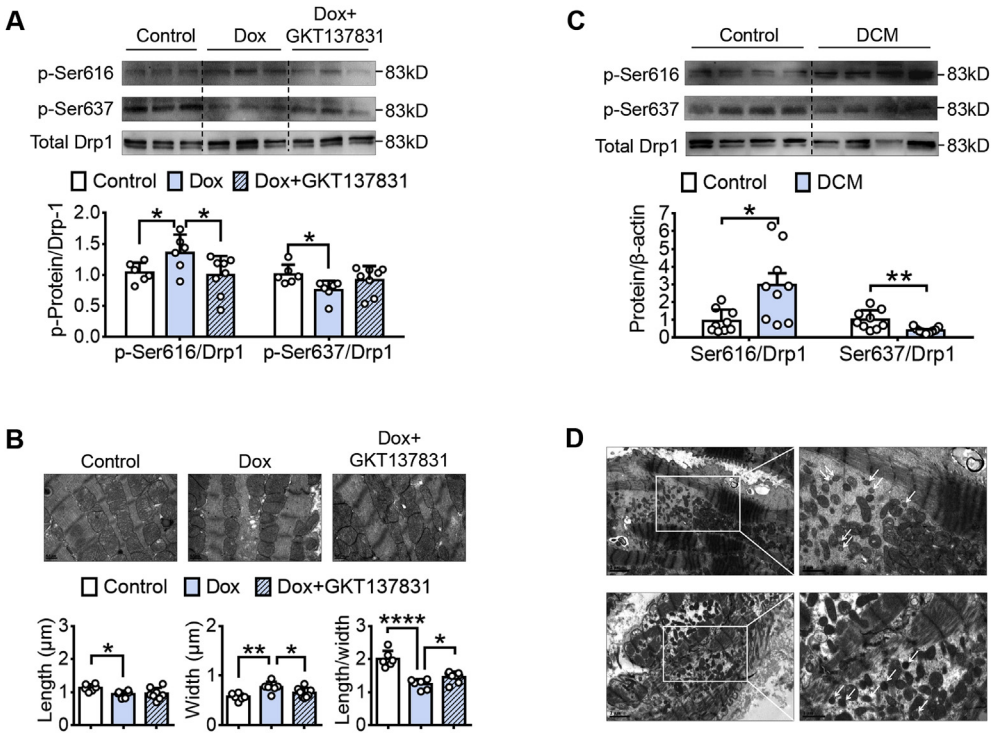


**Fig. 7. NOX1 and NOX4 facilitate Drp1 activation and mitochondrial fission in DCM**. (A and C) Representative immunoblots and the corresponding quantification of the expression and phosphorylation of Drp1 in Dox-induced DCM mice (n = 6–8) (A) and human DCM patients (n = 9) (C). (B) Mouse myocardial TEM images and quantitative analysis of mitochondrial length, width, and the ratio of length to width (n = 6–8). (D) Myocardial TEM images showing mitochondrial morphology of DCM patients. Note: besides the morphology of small spheroid mitochondria (white arrows), disrupted myofibrils, dispersed and disorganized mitochondria with abnormal internal membrane whorls and cristae lysis were also observed. $*p < 0.05$, $**p < 0.01$ and $****p < 0.0001$.

the alternative potential target for the therapies of chronic cardiomyopathy and HF.

Pyroptosis is associated with NLRP3 inflammasome activation. Although it was reported that mRNA levels of NLRP3 inflammasome components in peripheral blood mononuclear cells are higher in non-ischemic DCM patients than in healthy controls [33], no evidence of NLRP3 inflammasome activation is observed directly in cardiomyocytes of DCM hearts. Here we clearly present that NLRP3 inflammasome is activated in cardiomyocytes to mediate pyroptosis for DCM pathogenecity. Followed NLRP3 inflammasome activation, the mature forms of IL-1β and IL-18 release through the GSDMD pores, which may initiate and expand inflammation and result in cardiac injury in DCM. Particularly, depletion of pyroptosis by knocking out *NLRP3* or *caspase-1* attenuates cardiomyopathy and improves cardiac function in mice. This finding discloses that NLRP3 inflammasome activation and caspase-1-dependent pyroptosis can sufficiently cause the non-ischemic DCM.

*In vitro* study demonstrated that Dox activated NLRP3 inflammasomes in bone marrow-derived macrophages and H9c2 cells [34,35]. In our study, we further demonstrated that NLRP3 inflammasome is directly activated in Dox-treated non-immune primary rat cardiomyocytes. Moreover, we identified that Dox-stimulated cardiomyocytes show pyroptotic characters which are reversed by both caspase-1 and NLRP3 inflammasome inbibitors. These results reveal that Dox induces NLRP3 inflammasome-mediated pyroptosis via caspase-1 beyond immune cells, which is the potential cause to the direct myocardial damage.

Oxidative stress contributes to the progression of cardiomyopathy including DCM [36]. Accumulating evidence supported ROS plays central role in NLRP3 inflammasome activation [29]. NOXs are the major source of ROS in the cardiovascular system [37]. We manifested that the upregulations of NOX1 and NOX4, but not NOX2, are positively correlated with NLRP3 inflammasome activation and pyroptosis in myocardial tissues of DCM patients, and dual NOX1/NOX4 inhibitor efficiently attenuates NLRP3 inflammasome activation and pyroptosis, as well as the consequent cardiac dysfunction in DCM mice. Moreover, in consistent with our results in DCM patients and mice, inhibition of NOX1 and NOX4 suppressed pyroptotic cell death of cardiomyocytes induced by Dox. Our results disclosed for the first time that NOX1 and NOX4 play a novel role in DCM progression via NLRP3 inflammasome activation and cardiomyocyte pyroptosis, which also indicates that NOX1 and NOX4 are promising targets for preventing DCM. Compared with the general application of ROS scavenger, targeting a specific source of ROS may be a safe strategy for combating oxidative stress in HF [38]. The specific dual NOX1/NOX4 inhibitor, GKT137831, has been undergoing clinical evaluation for the treatment of diabetic nephropathy [39]. Our data presented that GKT137831 had potential clinical implications for DCM therapy.

We further disclosed that mitochondrial ROS is involved in Dox-induced NLRP3 inflammasome activation. Recent study demonstrated that mitochondrial fission contributed to excess mitochondrial ROS production in Dox-treated mice [40]. Drp1 is a ubiquitous protein for the dynamic regulation of mitochondrial fission. In response to cellular stress, the cytosolic Drp1 is translocated into mitochondria and promotes mitochondrial fission. Phosphorylation of Drp1 at Ser637 inhibits Drp1 activation and mitochondrial fission, whereas phosphorylation at Ser616 promotes mitochondrial fission [41,42]. In the present study, Dox changes the phosphorylation status of Drp1 both *in vivo* and *in vitro*, which mediates mitochondrial fission and leads to excess mitochondrial ROS production. Accordingly, Drp1 inhibitor decreases mitochondrial ROS, as well as NLRP3 inflammasome activation and cardiomyocyte pyroptosis. Especially, DCM patients show similar changes in Drp1 phosphorylation and mitochondrial morphology, supporting that Drp1-mediated mitochondrial fission plays an important role in the pathogenesis of DCM. Interestingly, dual NOX1/NOX4 inhibitor decreases Drp1-mediated mitochondrial fission, suggesting an upstream signaling of NOX1/NOX4 to mitochondria fission or mitochondria ROS release. However, the detailed mechanisms need to be further explored.

Taken together, our results demonstrate for the first time that cardiomyocyte pyroptosis triggered by NLRP3 inflammasome activation via caspase-1 causally contributes to myocardial dysfunction progression and DCM pathogenesis. We used a Dox-induced non-ischemic DCM as a model to uncover the novel role and underlying mechanism of NLRP3 inflammasome in cardiomyocyte pyroptosis for the occurrence of the non-ischemic DCM, which hints a possible cause of DCM, including myocarditis and exposure to alcohol, drugs and toxins, and

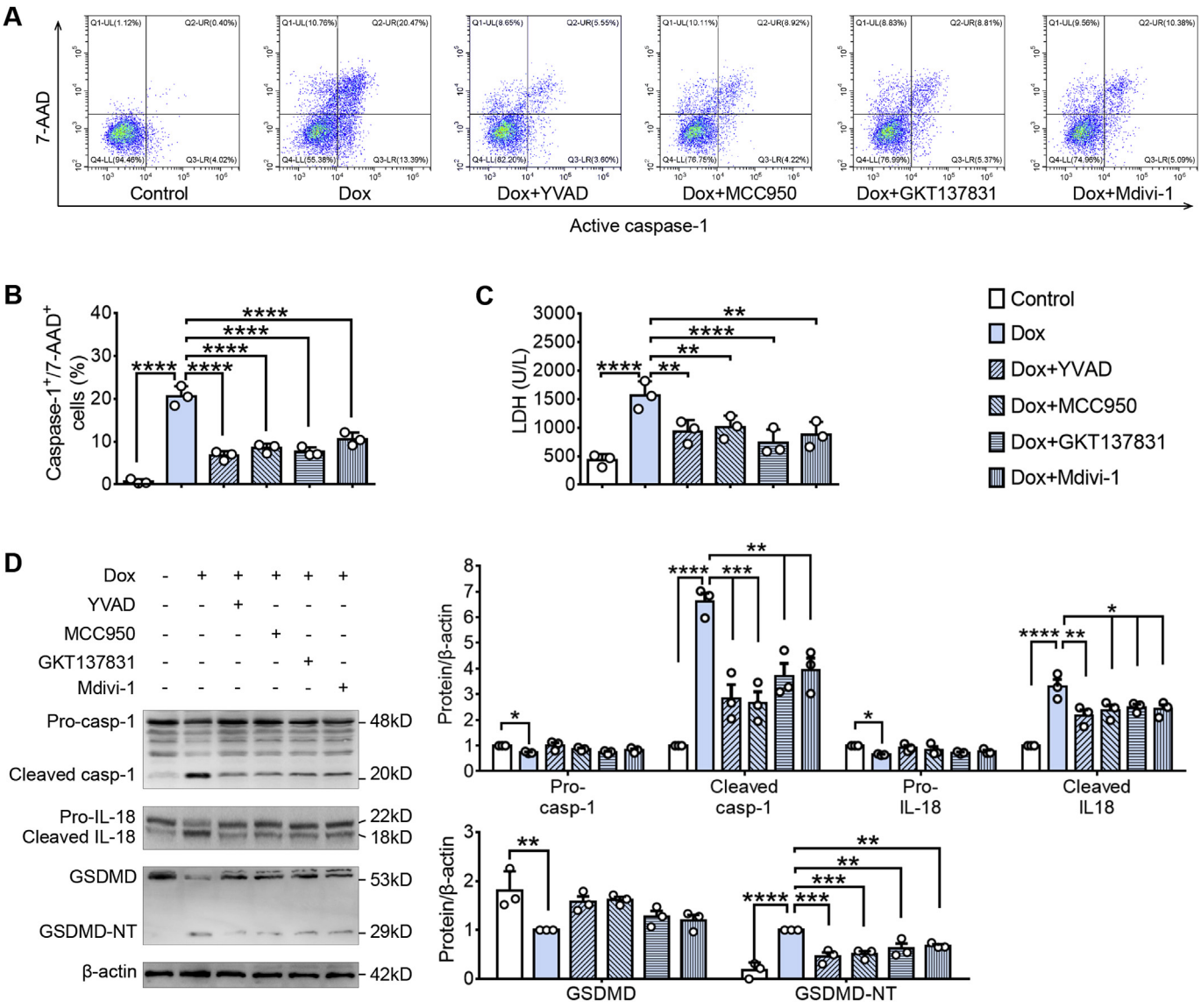


**Fig. 8. Targeting NOX1 and NOX4 or Drp1 reduced cardiomyocyte pyroptosis in primary NRVCs.** (A) Representative flow cytometric dot plots and (B) the corresponding quantification showing active caspase-$1^+$/7-$AAD^+$ cells as pyroptosis population (n = 3). (C) LDH levels in supernatant (n = 3). (D) Representative immunoblots and the corresponding quantification of the cleavage status of caspase-1, IL-18 and GSDMD (n = 3). $^*p < 0.05$, $^{**}p < 0.01$, $^{***}p < 0.001$ and $^{****}p < 0.0001$.

metabolic and endocrine disturbances. Expanding studies would be needed to characterize the detailed influences of the above factors in other DCM models. Given the current inefficiency in DCM therapy, targeting NLRP3 inflammasome or/and the related pyroptosis might be an effective alternative therapeutic strategy for chronic cardiomyopathy and HF.

## Author contributions

CZ and FD designed and performed research and collected, analyzed, and interpreted results. CZ prepared the first draft of the manuscript. JH, BL, BH, XL, and XS performed experiments. HL and XZ helped to establish the animal model. SY collected clinical parameter and tissues for patients, and interpreted results. HT obtained funding for the project, initiated and supervised the project, designed research, analyzed and interpreted results, and revised the manuscript. All authors reviewed the results and approved the final version of the manuscript.

## Declaration of competing interest

The authors have declared that no conflict of interest exists.

## Acknowledgments

This work was supported by the National Natural Science Foundation of China (grant numbers 81873514, 81570394 and 81370371) and Natural Science Foundation of Guangdong province (grant numbers 2017A030311017 and 2014A030313066).

## Appendix A. Supplementary data

Supplementary data to this article can be found online at https://doi.org/10.1016/j.redox.2020.101523.

## References

[1] R.G. Weintraub, C. Semsarian, P. Macdonald, Dilated cardiomyopathy, Lancet 390

(10092) (2017) 400–414.
[2] J. Narula, N. Haider, R. Virmani, T.G. DiSalvo, F.D. Kolodgie, R.J. Hajjar, U. Schmidt, M.J. Semigran, G.W. Dec, B.A. Khaw, Apoptosis in myocytes in end-stage heart failure, N. Engl. J. Med. 335 (16) (1996) 1182–1189.
[3] P. Di Napoli, A.A. Taccardi, A. Grilli, M. Felaco, A. Balbone, D. Angelucci, S. Gallina, A.M. Calafiore, R. De Caterina, A. Barsotti, Left ventricular wall stress as a direct correlate of cardiomyocyte apoptosis in patients with severe dilated cardiomyopathy, Am. Heart J. 146 (6) (2003) 1105–1111.
[4] W. Ibe, A. Saraste, S. Lindemann, S. Bruder, M. Buerke, H. Darius, K. Pulkki, L.M. Voipio-Pulkki, Cardiomyocyte apoptosis is related to left ventricular dysfunction and remodelling in dilated cardiomyopathy, but is not affected by growth hormone treatment, Eur. J. Heart Fail. 9 (2) (2007) 160–167.
[5] B.T. Cookson, M.A. Brennan, Pro-inflammatory programmed cell death, Trends Microbiol. 9 (3) (2001) 113–114.
[6] C. Zeng, R. Wang, H. Tan, Role of pyroptosis in cardiovascular diseases and its therapeutic implications, Int. J. Biol. Sci. 15 (7) (2019) 1345–1357.
[7] M. Magna, D.S. Pisetsky, The role of cell death in the pathogenesis of SLE: is pyroptosis the missing link? Scand. J. Immunol. 82 (3) (2015) 218–224.
[8] C. Yao, T. Veleva, L. Scott Jr., S. Cao, L. Li, G. Chen, P. Jeyabal, X. Pan, K.M. Alsina, I.D. Abu-Taha, S. Ghezelbash, C.L. Reynolds, Y.H. Shen, S.A. LeMaire, W. Schmitz, F.U. Muller, A. El-Armouche, N. Tony Eissa, C. Beeton, S. Nattel, X.H.T. Wehrens, D. Dobrev, N. Li, Enhanced cardiomyocyte NLRP3 inflammasome signaling promotes atrial fibrillation, Circulation 138 (20) (2018) 2227–2242.
[9] S. Toldo, A. Abbate, The NLRP3 inflammasome in acute myocardial infarction, Nat. Rev. Cardiol. 15 (4) (2018) 203–214.
[10] M. Takahashi, NLRP3 inflammasome as a novel player in myocardial infarction, Int. Heart J. 55 (2) (2014) 101–105.
[11] E. Mezzaroma, C. Marchetti, S. Toldo, Letter by Mezzaroma, et al regarding article, "NLRP3 inflammasome as a therapeutic target in myocardial infarction, Int. Heart J. 55 (4) (2014) 379.
[12] T. Strowig, J. Henao-Mejia, E. Elinav, R. Flavell, Inflammasomes in health and disease, Nature 481 (7381) (2012) 278–286.
[13] J. Shi, Y. Zhao, K. Wang, X. Shi, Y. Wang, H. Huang, Y. Zhuang, T. Cai, F. Wang, F. Shao, Cleavage of GSDMD by inflammatory caspases determines pyroptotic cell death, Nature 526 (7575) (2015) 660–665.
[14] Y. Naito, T. Tsujino, Y. Fujioka, M. Ohyanagi, H. Okamura, T. Iwasaki, Increased circulating interleukin-18 in patients with congestive heart failure, Heart 88 (3) (2002) 296–297.
[15] F.I. Parthenakis, A. Patrianakos, V. Prassopoulos, E. Papadimitriou, D. Nikitovic, N.S. Karkavitsas, P.E. Vardas, Relation of cardiac sympathetic innervation to proinflammatory cytokine levels in patients with heart failure secondary to idiopathic dilated cardiomyopathy, Am. J. Cardiol. 91 (10) (2003) 1190–1194.
[16] L.C. Magnano, N. Martinez Cibrian, X. Andrade Gonzalez, X. Bosch, Cardiac complications of chemotherapy: role of prevention, Curr. Treat. Options Cardiovasc. Med. 16 (6) (2014) 312.
[17] Y.J. Hong, T.K. Kim, D. Hong, C.H. Park, S.J. Yoo, M.E. Wickum, J. Hur, H.J. Lee, Y.J. Kim, Y.J. Suh, A. Greiser, M.Y. Paek, B.W. Choi, Myocardial characterization using dual-energy CT in doxorubicin-induced DCM: comparison with CMR T1-mapping and histology in a rabbit model, JACC Cardiovasc. Imag. 9 (7) (2016) 836–845.
[18] Y. Iwata, H. Ohtake, O. Suzuki, J. Matsuda, K. Komamura, S. Wakabayashi, Blockade of sarcolemmal TRPV2 accumulation inhibits progression of dilated cardiomyopathy, Cardiovasc. Res. 99 (4) (2013) 760–768.
[19] S. Leontyev, F. Schlegel, C. Spath, R. Schmiedel, M. Nichtitz, A. Boldt, R. Rubsamen, A. Salameh, M. Kostelka, F.W. Mohr, S. Dhein, Transplantation of engineered heart tissue as a biological cardiac assist device for treatment of dilated cardiomyopathy, Eur. J. Heart Fail. 15 (1) (2013) 23–35.
[20] E.M. Mantawy, W.M. El-Bakly, A. Esmat, A.M. Badr, E. El-Demerdash, Chrysin alleviates acute doxorubicin cardiotoxicity in rats via suppression of oxidative stress, inflammation and apoptosis, Eur. J. Pharmacol. 728 (2014) 107–118.
[21] R.A. Thandavarayan, V.V. Giridharan, S. Arumugam, K. Suzuki, K.M. Ko, P. Krishnamurthy, K. Watanabe, T. Konishi, Schisandrin B prevents doxorubicin induced cardiac dysfunction by modulation of DNA damage, oxidative stress and inflammation through inhibition of MAPK/p53 signaling, PloS One 10 (3) (2015) e0119214.
[22] M. Li, V. Sala, M.C. De Santis, J. Cimino, P. Cappello, N. Pianca, A. Di Bona, J.P. Margaria, M. Martini, E. Lazzarini, F. Pirozzi, L. Rossi, I. Franco, J. Bornbaum, J. Heger, S. Rohrbach, A. Perino, C.G. Tocchetti, B.H.F. Lima, M.M. Teixeira, P.E. Porporato, R. Schulz, A. Angelini, M. Sandri, P. Ameri, S. Sciarretta, R.C.P. Lima-Junior, M. Mongillo, T. Zaglia, F. Morello, F. Novelli, E. Hirsch, A. Ghigo, Phosphoinositide 3-kinase gamma inhibition protects from anthracycline cardiotoxicity and reduces tumor growth, Circulation 138 (7) (2018) 696–711.
[23] Y.W. Chen, B. Pat, J.D. Gladden, J. Zheng, P. Powell, C.C. Wei, X. Cui, A. Husain, L.J. Dell'italia, Dynamic molecular and histopathological changes in the extracellular matrix and inflammation in the transition to heart failure in isolated volume overload, Am. J. Physiol. Heart Circ. Physiol. 300 (6) (2011) H2251–H2260.
[24] R. von Harsdorf, P.F. Li, R. Dietz, Signaling pathways in reactive oxygen species-induced cardiomyocyte apoptosis, Circulation 99 (22) (1999) 2934–2941.
[25] R. Wang, Y. Wang, N. Mu, X. Lou, W. Li, Y. Chen, D. Fan, H. Tan, Activation of NLRP3 inflammasomes contributes to hyperhomocysteinemia-aggravated inflammation and atherosclerosis in apoE-deficient mice, Lab. Invest. 97 (8) (2017) 922–934.
[26] E. Cantu, D.J. Lederer, K. Meyer, K. Milewski, Y. Suzuki, R.J. Shah, J.M. Diamond, N.J. Meyer, J.W. Tobias, D.A. Baldwin, V.M. Van Deerlin, K.M. Olthoff, A. Shaked, J.D. Christie, C. Investigators, Gene set enrichment analysis identifies key innate immune pathways in primary graft dysfunction after lung transplantation, Am. J. Transplant. 13 (7) (2013) 1898–1904.
[27] Z. Liu, L. Gan, Y. Xu, D. Luo, Q. Ren, S. Wu, C. Sun, Melatonin alleviates inflammasome-induced pyroptosis through inhibiting NF-kappaB/GSDMD signal in mice adipose tissue, J. Pineal Res. 63 (1) (2017) e12414.
[28] L.L. Zhang, S. Huang, X.X. Ma, W.Y. Zhang, D. Wang, S.Y. Jin, Y.P. Zhang, Y. Li, X. Li, Angiotensin(1-7) attenuated Angiotensin II-induced hepatocyte EMT by inhibiting NOX-derived H2O2-activated NLRP3 inflammasome/IL-1beta/Smad circuit, Free Radic. Biol. Med. 97 (2016) 531–543.
[29] A. Abderrazak, T. Syrovets, D. Couchie, K. El Hadri, B. Friguet, T. Simmet, M. Rouis, NLRP3 inflammasome: from a danger signal sensor to a regulatory node of oxidative stress and inflammatory diseases, Redox Biol. 4 (2015) 296–307.
[30] S. Glumac, S. Pejic, S. Kostadinovic, Z. Stojsic, J. Vasiljevic, Apoptosis in endomyocardial biopsies from patients with dilated cardiomyopathy, Folia Biol. 62 (5) (2016) 207–211.
[31] K. Labbe, M. Saleh, Cell death in the host response to infection, Cell Death Differ. 15 (9) (2008) 1339–1349.
[32] X. Wu, H. Zhang, W. Qi, Y. Zhang, J. Li, Z. Li, Y. Lin, X. Bai, X. Liu, X. Chen, H. Yang, C. Xu, Y. Zhang, B. Yang, Nicotine promotes atherosclerosis via ROS-NLRP3-mediated endothelial cell pyroptosis, Cell Death Dis. 9 (2) (2018) 171.
[33] B. Luo, F. Wang, B. Li, Z. Dong, X. Liu, C. Zhang, F. An, Association of nucleotide-binding oligomerization domain-like receptor 3 inflammasome and adverse clinical outcomes in patients with idiopathic dilated cardiomyopathy, Clin. Chem. Lab. Med. 51 (7) (2013) 1521–1528.
[34] K.A. Sauter, L.J. Wood, J. Wong, M. Iordanov, B.E. Magun, Doxorubicin and daunorubicin induce processing and release of interleukin-1beta through activation of the NLRP3 inflammasome, Canc. Biol. Ther. 11 (12) (2011) 1008–1016.
[35] Z. Tavakoli Dargani, D.K. Singla, Embryonic stem cell-derived exosomes inhibit doxorubicin-induced TLR4-NLRP3-mediated cell death-pyroptosis, Am. J. Physiol. Heart Circ. Physiol. 317 (2) (2019) H460–H471.
[36] D. Cesselli, I. Jakoniuk, L. Barlucchi, A.P. Beltrami, T.H. Hintze, B. Nadal-Ginard, J. Kajstura, A. Leri, P. Anversa, Oxidative stress-mediated cardiac cell death is a major determinant of ventricular dysfunction and failure in dog dilated cardiomyopathy, Circ. Res. 89 (3) (2001) 279–286.
[37] K.K. Griendling, D. Sorescu, M. Ushio-Fukai, NAD(P)H oxidase: role in cardiovascular biology and disease, Circ. Res. 86 (5) (2000) 494–501.
[38] Z. Ahmed, W.H. Tang, Pharmacologic strategies to target oxidative stress in heart failure, Curr. Heart Fail. Rep. 9 (1) (2012) 14–22.
[39] S. Altenhofer, K.A. Radermacher, P.W. Kleikers, K. Wingler, H.H. Schmidt, Evolution of NADPH oxidase inhibitors: selectivity and mechanisms for target engagement, Antioxidants Redox Signal. 23 (5) (2015) 406–427.
[40] Y. Xia, Z. Chen, A. Chen, M. Fu, Z. Dong, K. Hu, X. Yang, Y. Zou, A. Sun, J. Qian, J. Ge, LCZ696 improves cardiac function via alleviating Drp1-mediated mitochondrial dysfunction in mice with doxorubicin-induced dilated cardiomyopathy, J. Mol. Cell. Cardiol. 108 (2017) 138–148.
[41] A. Jahani-Asl, R.S. Slack, The phosphorylation state of Drp1 determines cell fate, EMBO Rep. 8 (10) (2007) 912–913.
[42] C.R. Chang, C. Blackstone, Dynamic regulation of mitochondrial fission through modification of the dynamin-related protein Drp1, Ann. N. Y. Acad. Sci. 1201 (2010) 34–39.